

The Value of MR Neurography for Evaluating Extraspinal Neuropathic Leg Pain: A Pictorial Essay

Kevin R. Moore, Jay S. Tsuruda, and Andrew T. Dailey

Summary: Fifteen patients with neuropathic leg pain referable to the lumbosacral plexus or sciatic nerve underwent high-resolution MR neurography. Thirteen of the patients also underwent routine MR imaging of the lumbar segments of the spinal cord before undergoing MR neurography. Using phased-array surface coils, we performed MR neurography with T1-weighted spin-echo and fat-saturated T2-weighted fast spin-echo or fast spin-echo inversion recovery sequences, which included coronal, oblique sagittal, and/or axial views. The lumbosacral plexus and/or sciatic nerve were identified using anatomic location, fascicular morphology, and signal intensity as discriminatory criteria. None of the routine MR imaging studies of the lumbar segments of the spinal cord established the cause of the reported symptoms. Conversely, MR neurography showed a causal abnormality accounting for the clinical findings in all 15 cases. Detected anatomic abnormalities included fibrous entrapment, muscular entrapment, vascular compression, posttraumatic injury, ischemic neuropathy, neoplastic infiltration, granulomatous infiltration, neural sheath tumor, postradiation scar tissue, and hypertrophic neuropathy.

Conventional techniques for MR imaging of the lumbar segments of the spinal cord are well described and provide an excellent initial imaging approach for patients with back and leg pain. Routine protocols for MR imaging of the lumbar segments of the spinal cord provide excellent visualization of the spinal axis, including the central canal and foramina, but do not show the extraforaminal ventral rami, lumbosacral plexus, or sciatic nerve well. Unfortunately, for the subgroup of patients with leg pain referable to the lumbosacral plexus or sciatic nerve, routine MR imaging of the lumbar segments of the spinal cord will not usually reveal the cause of the pain. Some of these patients have extraforaminal anatomic abnormalities that explain their

clinical findings, and for these patients, high-resolution MR neurography may identify the causative anatomic abnormalities. High-resolution MR neurography has been previously described as a sensitive technique for identifying and characterizing peripheral nerve abnormalities (1-4) and for surgical planning (4, 5). Explicit indications for ordering an MR neurographic study and selection criteria for patients who might benefit from MR neurography after negative results of routine MR imaging of the lumbar segments of the spinal cord is beyond the scope of this discussion. Readers interested in a detailed discussion of these topics are referred to an excellent review article by Maravilla and Bowen (6). MR neurography protocols use high-resolution T1-weighted MR imaging sequences to delineate anatomic detail and fat-suppressed T2-weighted or short tau inversion recovery MR imaging sequences to detect abnormal nerve signal intensity. The primary goals of MR neurography are to localize the site of a nerve "injury" and to delineate the causative abnormality so that treatment planning can be properly directed.



FIG 1. Section orientation and coverage. Coronal T1-weighted localizer image (280/14/1) indicates the sagittal oblique plane and coverage area for imaging the LS plexus and proximal sciatic nerve.

Address reprint requests to Kevin R. Moore, MD, Department of Radiology, Section of Neuroradiology, University of Utah School of Medicine, 50 N. Medical Drive, 1A-71 Salt Lake City, UT 84132.

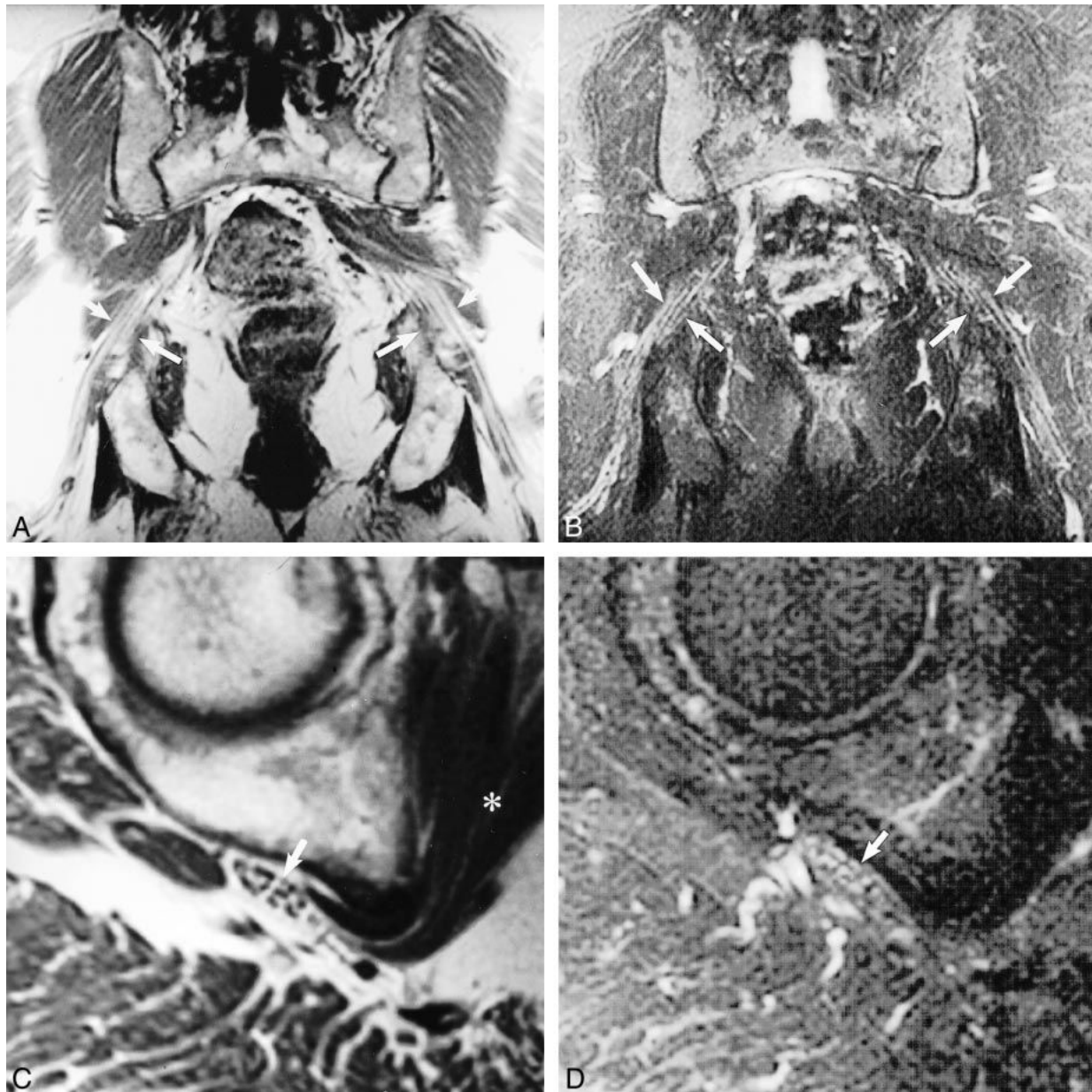


FIG 2. Normal sciatic nerve.

A, Coronal T1-weighted spin-echo image (600/10/2) illustrates the normal longitudinal fascicular appearance of the pelvic sciatic nerve (arrows).

B, T2-weighted fast spin-echo fat-saturated image (5200/102/3; echo train length, 8) shows normal sciatic nerve signal intensity (arrows).

C, Sagittal oblique plane T1-weighted image (550/9/2) depicts the characteristic transverse fascicular morphology of normal sciatic nerve (arrow) at the right obturator internus muscle level (asterisk).

D, Sagittal oblique plane T2-weighted fast spin-echo fat saturated image (5000/102/2; echo train length, 8), obtained at the same level as that shown in C, portrays normal sciatic nerve signal intensity (arrow). The T2 signal of normal nerve will be less intense than that of adjacent vessels and slightly hyperintense (occasionally isointense) to that of adjacent muscle.

Understanding the relevant lumbosacral plexus and sciatic nerve anatomy is crucial for the correct interpretation of MR neurographic studies. The lumbar plexus is composed of the ventral rami of L1 through L4 and is anatomically located behind the psoas muscle (7). A minor branch of L4 combines with the ventral ramus of L5 to form the lumbosacral trunk or cord (7). The lumbosacral trunk descends over the sacral ala and combines with the

ventral rami of S1, S2, and S3 (and a branch of S4) to form the sacral plexus (7). The individual sacral plexus neural components coalesce and diverge along the ventral piriformis muscle surface, making it the key anatomic landmark for locating the sacral plexus and sciatic nerve. The sciatic nerve originates from the upper division of the sacral plexus at the inferior piriformis muscle border, and exits the pelvis through the greater sciatic fo-

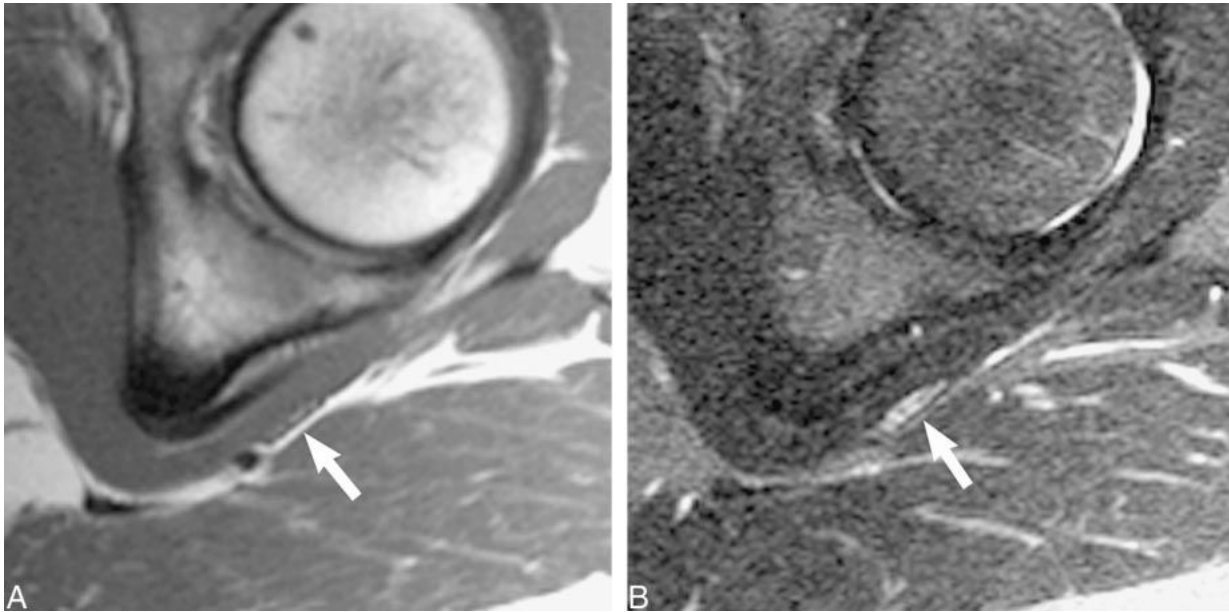


FIG 3. Compressive neuropathy.

A, Sagittal oblique plane T1-weighted image (680/14/3) reveals marked flattening of the left sciatic nerve (*arrow*) between hypertrophied obturator internus and gluteus maximus muscles. Note, however, that the transverse fascicular morphology is preserved.

B, Sagittal oblique plane fat-saturated T2-weighted fast spin-echo (6000/102/3; echo train length, 8) image, obtained at the same level as that shown in A, shows abnormally increased sciatic nerve T2 hyperintensity (*arrow*) that approaches regional vessel signal intensity.

ramen (7). The sciatic nerve gives rise to the tibial and common peroneal nerves, two anatomically and functionally distinct nerves that travel together in the thigh as the sciatic nerve. In most patients, the sciatic nerve bifurcates just above the knee into separate common peroneal and tibial nerves. We review the spectrum of abnormal neurographic findings that may be encountered in this clinically challenging patient population.

Description of the Technique

Patient Demographics

All 15 positive lumbosacral plexus or sciatic nerve MR neurograms obtained between July 1997 and July 1999 were reviewed by two neuroradiologists (K.R.M., J.S.T.). All patients had neuropathic leg symptoms referable to the lumbosacral plexus or sciatic nerve. Clinical information was obtained by medical chart review and discussion with referring physicians. All 15 patients (seven male and eight female patients; mean age, 39 years; age range, 11–68 years) underwent imaging with a high-resolution MR neurographic technique. Thirteen patients also underwent routine MR imaging of the lumbar segments of the spinal cord before undergoing MR neurography.

Prospective Delineation of Necessary Scan Coverage

Because MR neurography sequences are relatively lengthy and motion sensitive, it is not generally feasible to screen the whole extremity from nerve root to sciatic bifurcation in one sitting. Department scheduling constraints and limited patient tolerance for prolonged MR imaging generally limit imaging time to approximately 1 hour. Therefore, it is imperative to prospectively determine the most likely level of the abnormality before initiating imaging, using all available clinical and electrophysiological information. For most of the patients, the abnormality was clinically localized using pain distribution, presence of a palpable mass, and/or motor or sensory deficits

to determine the necessary coverage. Where available, electrophysiological studies, including electromyography and nerve conduction velocity studies, were used to limit the area examined. If electrophysiological studies were unavailable and the physical examination could not localize the abnormality to either the lumbosacral plexus or sciatic nerve, imaging was initiated proximally at the lumbosacral plexus and continued distally into the thigh by using multiple stations through the tibioperoneal bifurcation or until the causative abnormality was revealed.

MR Neurography Imaging Protocol

Detailed descriptions of MR neurography protocols have been previously published (1–4). Readers interested in a comprehensive discussion of MR peripheral nerve imaging technique are directed to the review article by Maravilla and Bowen (6). High-resolution peripheral nerve imaging requires careful consideration of coil selection, pulse sequence, method of fat suppression, section thickness, and field of view (6). Successful identification of subtle nerve abnormalities by use of MR neurography requires that the imaging parameters be optimized to maximize the signal-to-noise ratio, that spatial and contrast resolution sufficient to permit accurate delineation of fascicular morphology and nerve signal intensity be produced, and that a reasonable imaging time be maintained. We have found that a thoracic wrap-around phase-array coil placed over the pelvis or thighs provides optimal coverage of the lumbosacral plexus and sciatic nerve. Pelvic phase-array coils provide satisfactory coverage of the lumbosacral plexus but are inadequate for examining the sciatic nerve in most patients.

All MR neurographic studies were performed on 1.5-T MR imagers (Signa; GE Medical Systems, Milwaukee, WI), using a thoracic wrap-around (Medical Advances, Milwaukee, WI) or pelvis phase-array (GE Medical Systems) coil. Shared parameters common to all sequences included 4- to 7-mm section thickness, 0-mm intersection gap, 18- to 24-cm field of view, 256 × 192 to 256 matrix, and an 8- to 10-minute imaging time per sequence. All patients underwent coronal-view T1-weighted spin-echo (550–800/10–15/2–3 [TR/TE/excitations]) and

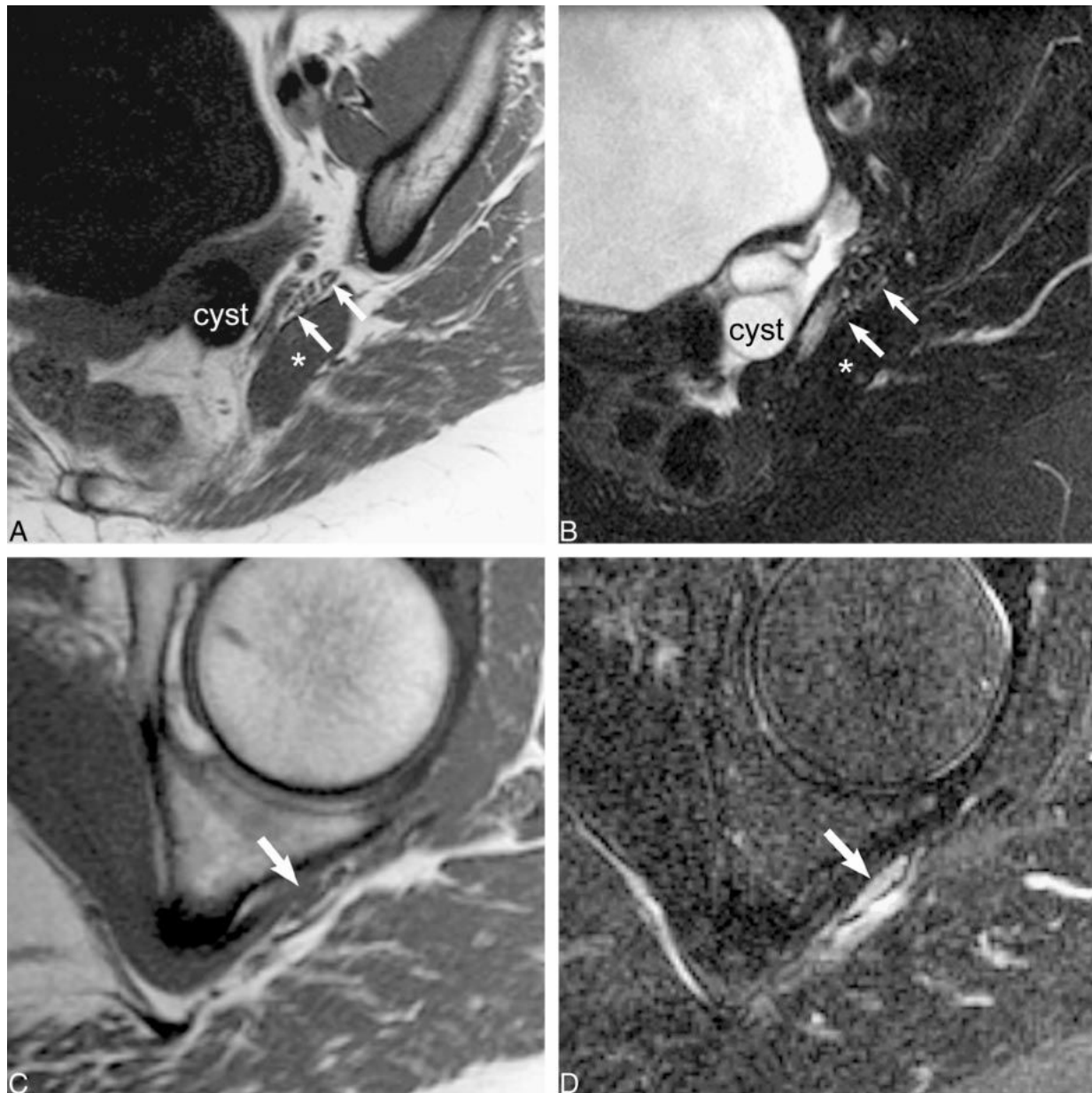


FIG 4. Traumatic neuropathy.

A, Sagittal oblique plane T1-weighted image (560/10/2), obtained at the level of the piriformis muscle (*asterisk*), reveals normal size and fascicular morphology of the left sciatic nerve (*arrows*). The adjacent adnexal cyst (*cyst*) approximates but does not distort or displace the normal sciatic nerve.

B, Sagittal oblique plane fat-saturated T2-weighted fast spin-echo image (4000/108/2; echo train length, 8), obtained at the same level as that shown in A, confirms normal nerve signal intensity (*arrows*).

C, Sagittal oblique plane T1-weighted image (560/10/2), obtained at the level of the obturator internus muscle, reveals flattening of the left sciatic nerve and disruption of the normal transverse fascicular pattern (*arrow*).

D, Sagittal oblique plane fat-saturated T2-weighted fast spin-echo image (4000/108/2; echo train length, 8), obtained at the same level as that shown in C, shows abnormal sciatic nerve hyperintensity (*arrow*) equivalent to that of regional vessels. Unlike the case illustrated in Figure 3, there is no identifiable mechanical compressive cause in this case.

either fast spin-echo inversion recovery (4600–5000/45/2–3; inversion time, 160 ms; echo train length, 8), or fat-saturated T2-weighted fast spin-echo (4000–6000/95–105/2–3; echo train length, 8) sequences, with imaging coverage from L3 through the ischial tuberosity centered in the midline. Using a longer TE (45 ms) on the fast spin-echo inversion recovery sequences provides excellent muscle signal suppression. Patients whose abnormalities were clinically localizing to the lumbosacral plexus underwent additional axial-view T1-weighted spin-echo and fat-saturated T2-weighted fast spin-

echo or fast spin-echo inversion recovery imaging from L3 through the ischial tuberosity, centered in the midline. Patients whose abnormalities were clinically localizing to the proximal sciatic nerve underwent additional sagittal-view oblique-plane T1-weighted spin-echo and T2-weighted fast spin-echo fat-saturated or fast spin-echo inversion recovery imaging on the symptomatic side, from the sacral ala through the ischial tuberosity (Fig 1). Patients whose abnormalities were localizing to the sciatic nerve in the thigh underwent additional axial-view T1-weighted spin-echo and T2-weighted fast spin-echo



FIG 5. Hypertrophic neuropathy.

A, Axial T1-weighted image (600/20/2) shows the sciatic nerve in the left proximal thigh. The tibial division reveals a central mass (*white arrow*) that is isointense to muscle and that displaces several mildly swollen fascicles to the nerve periphery. The peroneal division (*black arrow*) appears normal at this level.

B, Axial fast spin-echo inversion recovery image (4600/45/2; echo train length, 8), obtained at the same level as that shown in A, shows normal peroneal division morphology and signal intensity (*black arrow*). More distally (not shown), the peroneal division manifested abnormal T2 hyperintensity, reflecting a compressive neuropraxic injury that explained the foot drop. The central tibial nerve mass displaces several mildly swollen hyperintense fascicles to the periphery (*white arrow*).

C, Axial contrast-enhanced T1-weighted image (550/14/2) shows modest enhancement of the central tibial division mass (*white arrow*). There is no abnormal enhancement of the adjacent peroneal division (*black arrow*).

fat-saturated imaging on the symptomatic side from the ischial tuberosity to the tibioperoneal bifurcation. In all cases, the field of view was reduced as small as possible while maintaining adequate signal-to-noise ratio and avoiding phase wrap. Contrast-enhanced fat-saturated T1-weighted imaging was performed when a mass lesion or postoperative scar was suspected to be the cause of the symptom and when a mass or scar was identified on an unenhanced imaging sequence.

Protocols for Routine MR Imaging of the Lumbar Segments of the Spinal Cord

Thirteen patients also underwent routine MR imaging of the lumbar segments of the spinal cord on 1.5-T MR imagers (Signa). Imaging sequences included sagittal-view T1-weighted spin-echo (550/16/2; matrix, 256 × 256; field of view, 24 cm; section thickness, 4.0 mm; section gap, 1.0 mm), sagittal-view T2-weighted fast spin-echo (3000/80/4; echo train length, 16; matrix, 512 × 256; field of view, 24 cm; section thickness, 4.0 mm; section gap, 1.0 mm), and axial-view short (3650/17/

2) and long (3650/102/2) TE sequences (echo train length, 8; matrix, 256 × 256; field of view, 18 cm; sections thickness, 4.0 mm; section gap, 0.0 mm).

Criteria for Determining Normal versus Abnormal Study Results

The normal appearance of the sciatic nerve has been described (1, 2, 4, 6). The normal sciatic nerve (Fig 2) is a well-defined oval structure with discrete fascicles isointense to adjacent muscle tissue on T1-weighted images. Normal nerve fascicles should be of uniform size and shape. On T2-weighted or fast spin-echo inversion recovery images, the normal sciatic nerve is slightly hyperintense to adjacent muscle and hypointense to regional vessels, with clearly defined fascicles separated by interposed lower signal connective tissue. Study results were considered to be normal if the sciatic nerve or lumbosacral plexus was of normal size and had fascicular architecture on the T1-weighted images and had normal signal

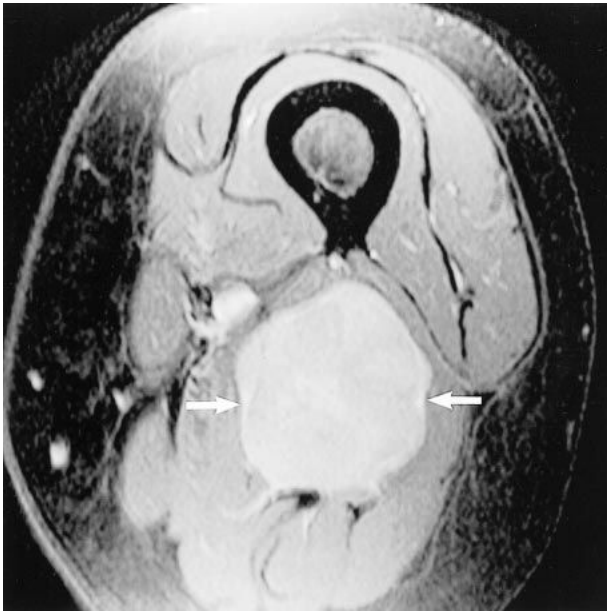


FIG 6. Metastatic dermatofibrosarcoma. Axial contrast-enhanced T1-weighted fat-saturated image (600/9/2), obtained through the distal left thigh, reveals a 3-cm enhancing mass (arrows) centered within the sciatic nerve. Surgical resection revealed metastatic dermatofibrosarcoma.

intensity on the T2-weighted or fast spin-echo inversion recovery images (Fig 2).

The interpretation criteria for positive results of an MR neurography study included focal nerve enlargement or distortion of normal fascicular morphology on T1-weighted sequences and hyperintensity of the questioned nerve on the T2-weighted or fast spin-echo inversion recovery sequences. In general, positive study results show nerve T2-weighted signal intensity approaching that of regional blood vessels. Because of time constraints and the necessity to limit the fields of view, only the symptomatic side was studied in the sagittal oblique plane. Both sides underwent imaging in the coronal plane. Determination that a sciatic nerve was abnormal was based on side-to-side comparison of the coronal sequences and comparison to normal sagittal oblique plane studies from our institutional database of normal MR neurograms.

Illustrative Clinical Material

The anatomic abnormalities discovered were myriad and included muscle or fibrous sciatic nerve compressive entrapment neuropraxia (three cases), traumatic neuropraxic sciatic nerve injury (two cases), amputation stump traumatic neuroma (one case), presumed ischemic S2 neuropathy (one case), postradiation scar tissue (one case), sciatic sarcoidosis (one case), sciatic hypertrophic neuropathy (one case), giant iliac fossa L5 ventral ramus schwannoma (one case), plexiform neurofibroma (one case), and neoplastic infiltration (three cases). Selected illustrative cases are presented.

Compressive Neuropathy

A 20-year-old male bodybuilder, said to have prominent development of his buttock musculature, presented with intractable left sciatica and loss of lower extremity muscle mass. Palpation over the left buttock exacerbated pain. Based on physical examination, a working clinical diagnosis of "piriformis syndrome" was made. Routine MR imaging of the lumbar segments of the spinal cord was noncontributory. MR neurography showed normal morphology and signal intensity at

the piriformis muscle level. Conversely, the sciatic nerve was markedly hyperintense and flattened between the hypertrophied obturator internus and gluteus maximus muscles, with maintenance of recognizable fascicular anatomy (Fig 3). Conservative management was elected.

Traumatic Neuropathy

A 46-year-old woman fell while skiing and presented with persistent left buttock and leg pain in the sciatic nerve distribution, which was unresponsive to conservative management. On the basis of clinical examination and normal routine MR imaging of the lumbar segments of the spinal cord, a working diagnosis of piriformis syndrome was made. An adnexal cyst was incidentally noted adjacent to the left sciatic nerve at the piriformis level on the routine MR imaging study of the lumbar segments of the spinal cord. Although thought to be unlikely, nerve compression by the cyst was considered as a possible cause, and laparoscopic cyst resection was considered. The patient elected further conservative management, but physical therapy and nerve root and piriformis muscle injections produced no symptomatic improvement. She was referred for MR neurography to further elucidate the relationship between the adnexal cyst and sciatic nerve at the piriformis level. No signal abnormality or architectural sciatic nerve distortion was observed adjacent to the cyst at the piriformis muscle (Fig 4A and B). However, at the obturator internus and superior gemellus muscles, MR neurography revealed mild enlargement and focal T2 hyperintensity of the left sciatic nerve (Fig 4C and D) without macroscopic muscular compression. On the basis of MR neurographic study, surgical management was excluded, and the patient elected continued physical therapy directed toward the hip adductor and abductor musculature.

Hypertrophic Neuropathy

A 28-year-old woman with a clinical diagnosis of S1 radiculopathy presented with left leg weakness localized to the gastrocnemius and soleus muscles. The results of routine MR imaging of the lumbar segments of the spinal cord were normal. The patient's condition failed to improve with conservative management, and she subsequently developed an additional left foot drop. Based on clinical findings, the level of sciatic nerve abnormality was predicted to be in the thigh above the tibioperoneal bifurcation. Directed MR neurography (Fig 5) revealed an infiltrating 11-cm-long enhancing sciatic nerve mass centered within the tibial division, extending from the ischial tuberosity to the tibioperoneal bifurcation. Several enlarged peripherally displaced tibial division fascicles displayed abnormally elevated T2 hyperintensity. The distal sciatic nerve (peroneal division) revealed abnormal elevated T2 signal intensity (not shown), but preserved fascicular morphology, implying a compressive neuropraxic injury as the mechanism for the foot drop. The preoperative diagnosis was schwannoma. Open biopsy revealed fibrosis and "onion bulb" lesions, characteristic of hypertrophic neuropathy, and a surgical internal neurolysis of the mid-thigh sciatic nerve was performed. The attending neurosurgeon noted poor anatomic delineation of individual nerve fascicles at the time of surgery. The patient achieved improved motor strength after surgery and had maintained the improvement at the 1-year follow-up visit.

Metastatic Dermatofibrosarcoma

A 48-year-old woman with dermatofibrosarcoma protuberans and multiple soft-tissue and visceral metastatic lesions presented with new progressive distal left leg weakness and pain. A physical examination revealed zero of five strength in muscles supplied by both the tibial and common peroneal nerves. Routine MR imaging of the lumbar segments of the spinal cord

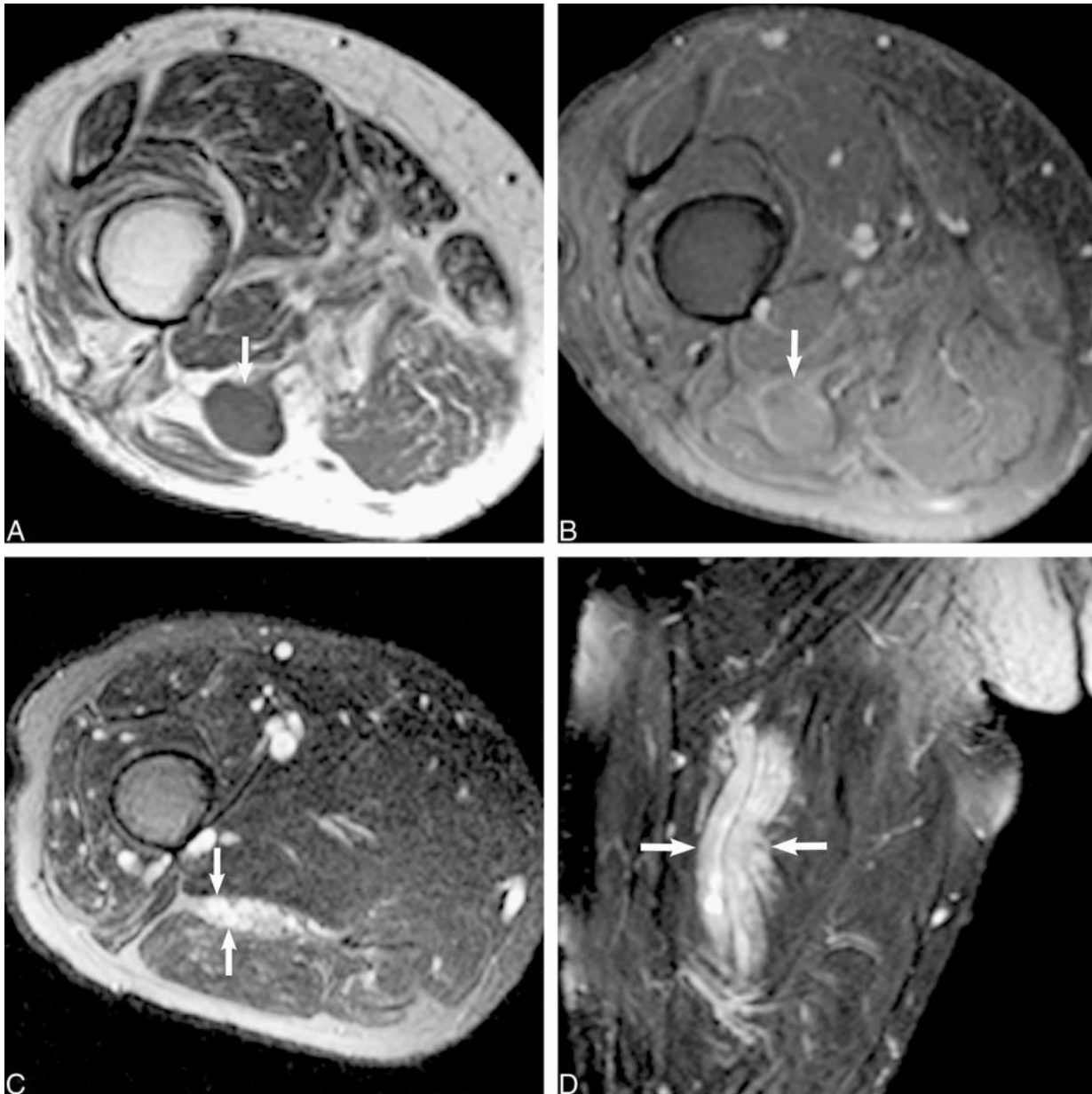


FIG 7. Traumatic stump neuroma.

A, Axial T1-weighted spin-echo image (600/9/2), obtained through the right distal thigh (stump), reveals a low signal intensity mass (arrow) within the distal sciatic nerve.

B, Axial T1-weighted spin-echo contrast-enhanced fat-saturated image (550/14/2) shows mild enhancement of the mass (arrow).

C, Axial T2-weighted fast spin-echo fat-saturated image (5000/90/2; echo train length, 8), obtained proximal to the mass, shows sciatic nerve enlargement with focal swollen T2-weighted hyperintense fascicles (arrows).

D, Coronal T2-weighted fast spin-echo fat-saturated image (5000/102/2; echo train length, 8) confirms diffuse sciatic nerve enlargement and abnormal T2 hyperintensity (arrows) proximal to the mass. Final surgical pathologic analysis revealed traumatic neuroma.

revealed no anatomic explanation. Based on clinical localization to the thigh level, MR neurography was performed through the distal thigh and revealed a 3.5-cm soft-tissue mass with signal intensity and enhancement characteristics similar to those of the patient's other metastatic lesions centered within the sciatic nerve (Fig 6). Surgical internal debulking revealed metastatic dermatofibrosarcoma diffusely infiltrating both the tibial and common peroneal nerve fascicles. Postoperatively, no motor strength improvement was noted, but the patient did experience a marked reduction in dysesthetic leg pain that persisted at the 6-month follow-up visit.

Traumatic Stump Neuroma

A previously well 53-year-old man with neurofibromatosis type 1 presented 30 years after traumatic above-the-knee amputation with new phantom limb pain after a fall. Routine MR imaging of the lumbar segments of the spinal cord revealed tiny right L4 and S2 nerve root neurofibromas that were deemed unlikely to be causative of the symptoms. On the basis of pain and a positive Tinel's sign localized to the stump level, MR neurography was performed through the right thigh and revealed an enhancing 1.5-cm \times 1.5-cm mass in the distal stump (Fig 7). Proximal to the mass, the sciatic nerve was

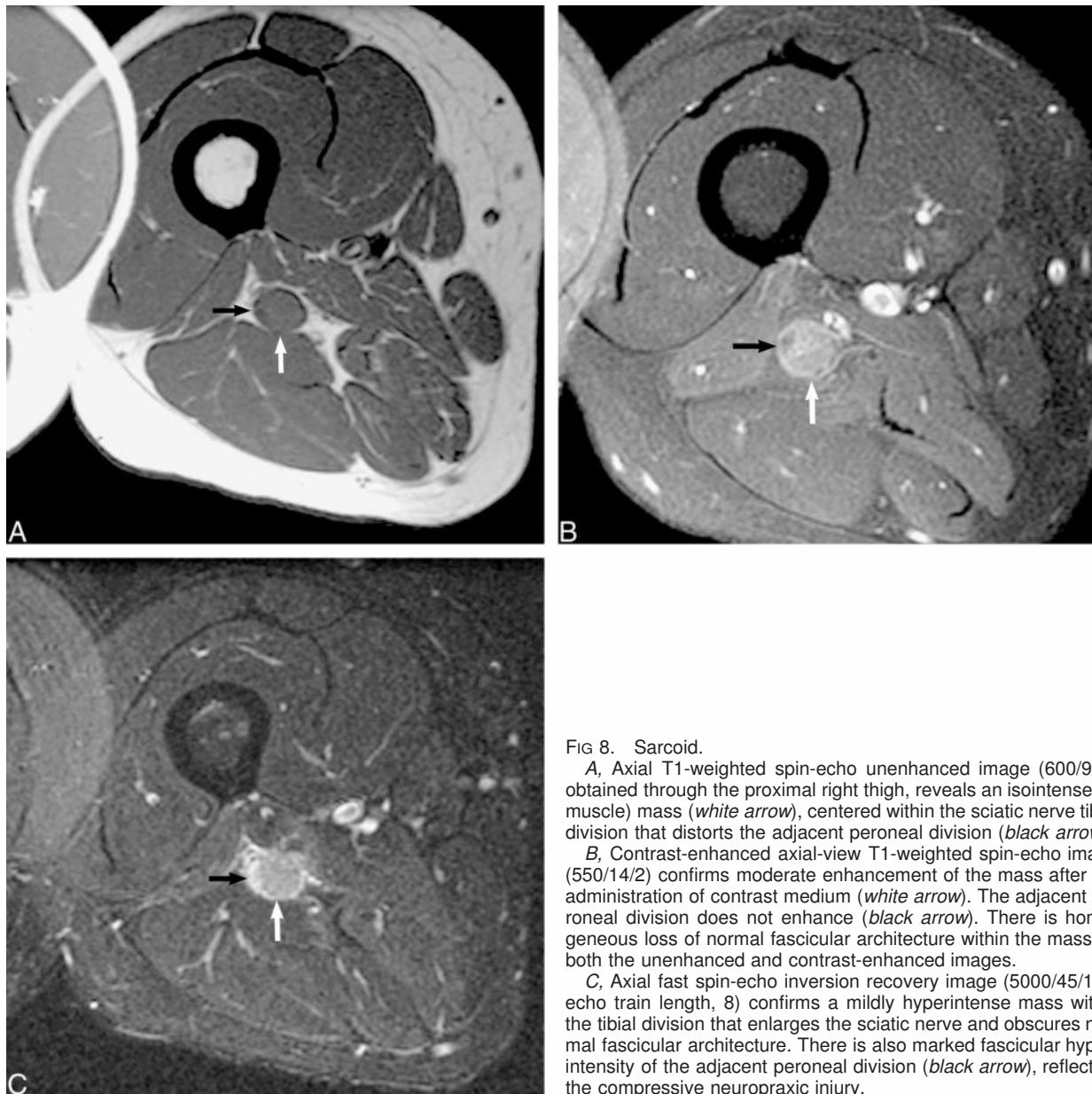


FIG 8. Sarcoid.

A, Axial T1-weighted spin-echo unenhanced image (600/9/2), obtained through the proximal right thigh, reveals an isointense (to muscle) mass (*white arrow*), centered within the sciatic nerve tibial division that distorts the adjacent peroneal division that (*black arrow*).

B, Contrast-enhanced axial-view T1-weighted spin-echo image (550/14/2) confirms moderate enhancement of the mass after the administration of contrast medium (*white arrow*). The adjacent peroneal division does not enhance (*black arrow*). There is homogeneous loss of normal fascicular architecture within the mass on both the unenhanced and contrast-enhanced images.

C, Axial fast spin-echo inversion recovery image (5000/45/150; echo train length, 8) confirms a mildly hyperintense mass within the tibial division that enlarges the sciatic nerve and obscures normal fascicular architecture. There is also marked fascicular hyperintensity of the adjacent peroneal division (*black arrow*), reflecting the compressive neuropraxic injury.

enlarged with marked focal fascicular enlargement and increased T2 hyperintensity. The preoperative diagnosis of post-traumatic neuroma was confirmed at surgery. The patient remained symptom-free after resection.

Sciatic Nerve Sarcoidosis

A 22-year-old woman presented with multiple neurologic complaints, including right leg pain and weakness. MR imaging of the brain and spinal axis to exclude multiple sclerosis revealed nothing abnormal. A clinical examination revealed weakness of the right leg posterior compartment muscles but no palpable leg mass. Sciatic nerve MR neurography through the thigh revealed a mildly enhancing 6-cm-long mass centered within the tibial division (Fig 8). The mass was hypointense on T1-weighted images. T2-weighted imaging revealed fascicular enlargement proximal and distal to the mass. On the basis of homogeneous loss of normal fascicular architecture at the mass level and enhancement characteristics, a preoperative diagnosis of neurofibroma was made. Surgical internal neuroly-

sis and biopsy revealed chronic inflammatory changes and multinucleated giant cells with noncaseating granulomas, characteristic of sarcoidosis.

Conclusion

Patients with unrelenting leg pain and nonspecific results of routine MR imaging studies of the lumbar segments of the spinal cord are commonly encountered in clinical practice. The vast majority of patients with neurogenic leg pain have causative abnormalities in the lumbosacral spine, most frequently disk disease, compressive osteophytes, or central canal stenosis. However, within this population is a subgroup of patients who seek medical attention because of symptoms and correlating clinical signs referable to the lumbosacral plexus or

sciatic nerve. Although routine protocols for MR imaging of the lumbar segments of the spinal cord are helpful for evaluating the majority of patients with back or leg pain who require imaging, they do not adequately examine either the lumbosacral plexus or sciatic nerve. Therefore, for patients with neuropathic leg pain resulting from extraforaminal lesions, the cause of the pain generally will not be revealed by routine MR imaging of the lumbar segments of the spinal cord. Conversely, MR neurography is a sensitive diagnostic imaging technique for evaluating both the lumbosacral plexus and sciatic nerve. Tailored high-resolution MR neurography of these selected patients with unexplained sciatica may reveal a causative abnormality not detected by routine MR imaging of the lumbar segments of the spinal cord and can redirect subsequent clinical treatment. The spectrum of abnormal plexus and sciatic nerve anatomic findings is myriad and includes fibrous entrapment, muscular entrapment, vascular compression, posttraumatic le-

sions, ischemic neuropathy, neoplastic infiltration, granulomatous infiltration, neural sheath tumor, postradiation scar tissue, and hypertrophic neuropathy.

References

1. Filler AG, Kliot M, Howe FA, et al. **Application of magnetic resonance neurography in the evaluation of patients with peripheral nerve pathology.** *J Neurosurg* 1996;85:299-309
2. Maravilla K, Aagaard B, Kliot M. **MR neurography: MR imaging of peripheral nerves.** *Magn Reson Imaging Clin N Am* 1998;6:179-194
3. Filler AG, Howe FA, Hayes CE, et al. **Magnetic resonance neurography.** *Lancet* 1993;341:659-661
4. Kuntz C IV, Blake L, Britz G, et al. **Magnetic resonance neurography of peripheral nerve lesions in the lower extremity.** *Neurosurgery* 1996;39:750-757
5. Grant GA, Goodkin R, Kliot M. **Evaluation and surgical management of peripheral nerve problems.** *Neurosurgery* 1999;44:825-840
6. Maravilla KR, Bowen BC. **Imaging of the peripheral nervous system: evaluation of peripheral neuropathy and plexopathy.** *AJNR Am J Neuroradiol* 1998;19:1011-1023
7. Pick T, Howden R, eds. *Anatomy, Descriptive and Surgical (Gray's Anatomy)*. Philadelphia: Running Press;1974:781-793